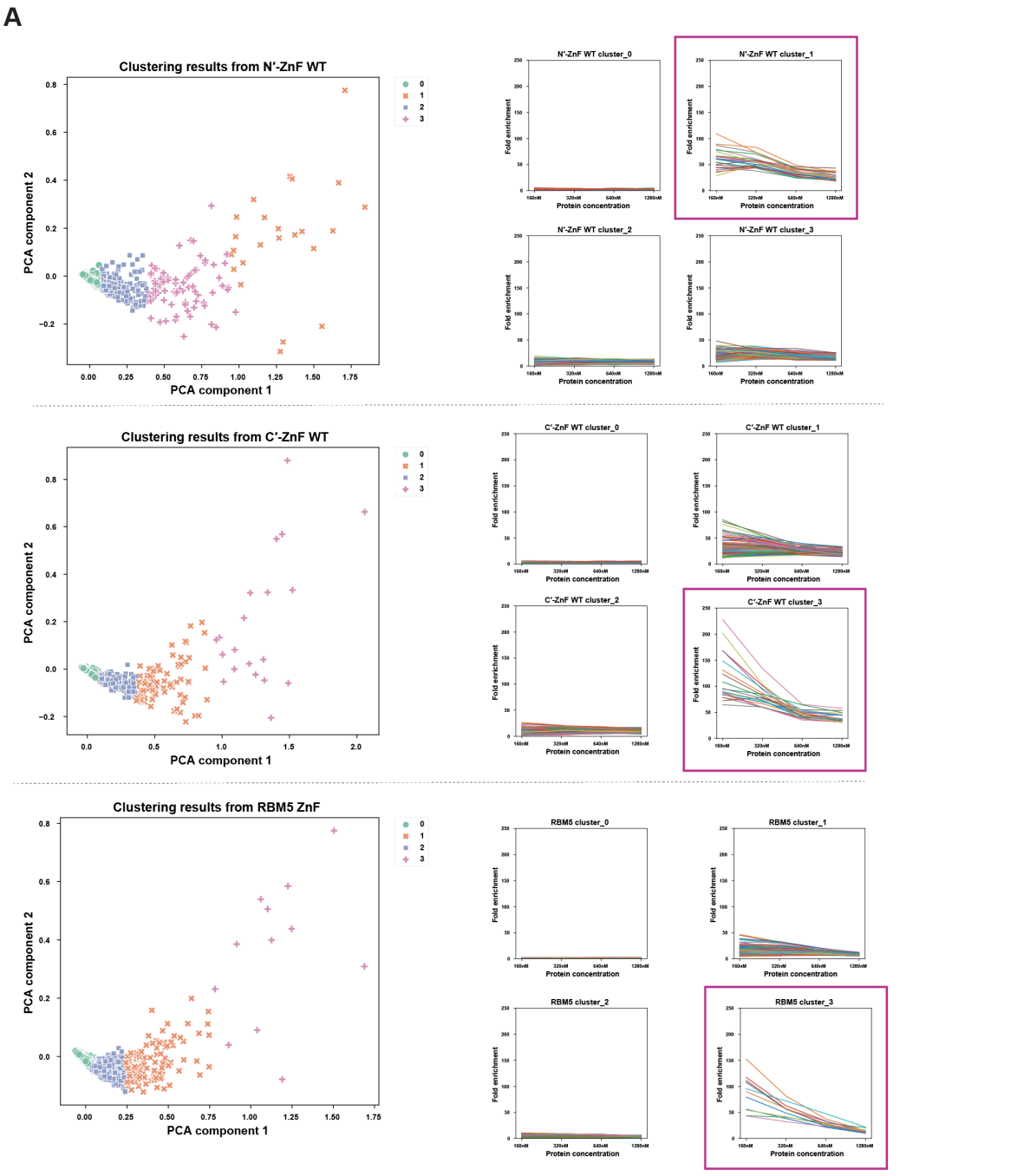

Supplemental Figure S1: Benchmarking of the modified RNA bind-n-seq (RBNS) assay
(A) K-mean clustering of RNA 6-mers based on their fold enrichment in the benchmarking RBNS experiments. Red box: signature cluster, defined as the RNA 6-mers with distinct binding affinities to the protein at low protein concentration. (B) Fraction of sequence motifs containing GGU or GGG in the signature cluster in the benchmarking RBNS experiments,

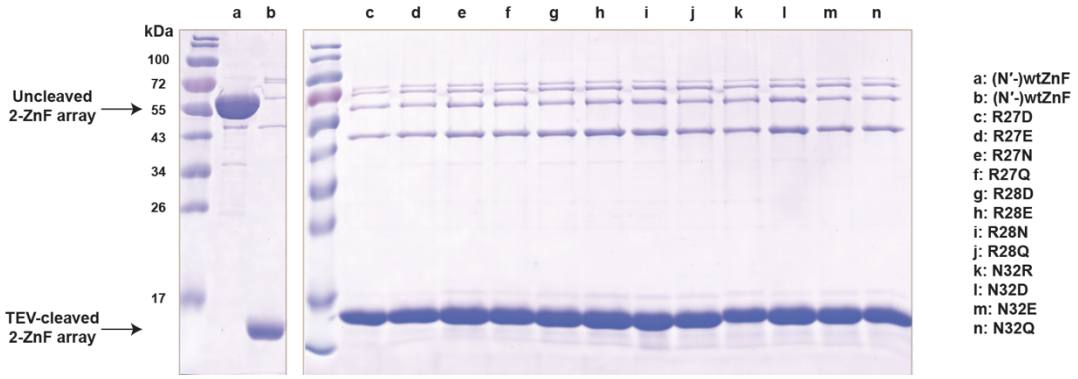

Supplemental Figure S2: Purification of single mutant ZnF-array
Representative SDS-PAGE gel image of the high-throughput purification of single mutant ZnF arrays.

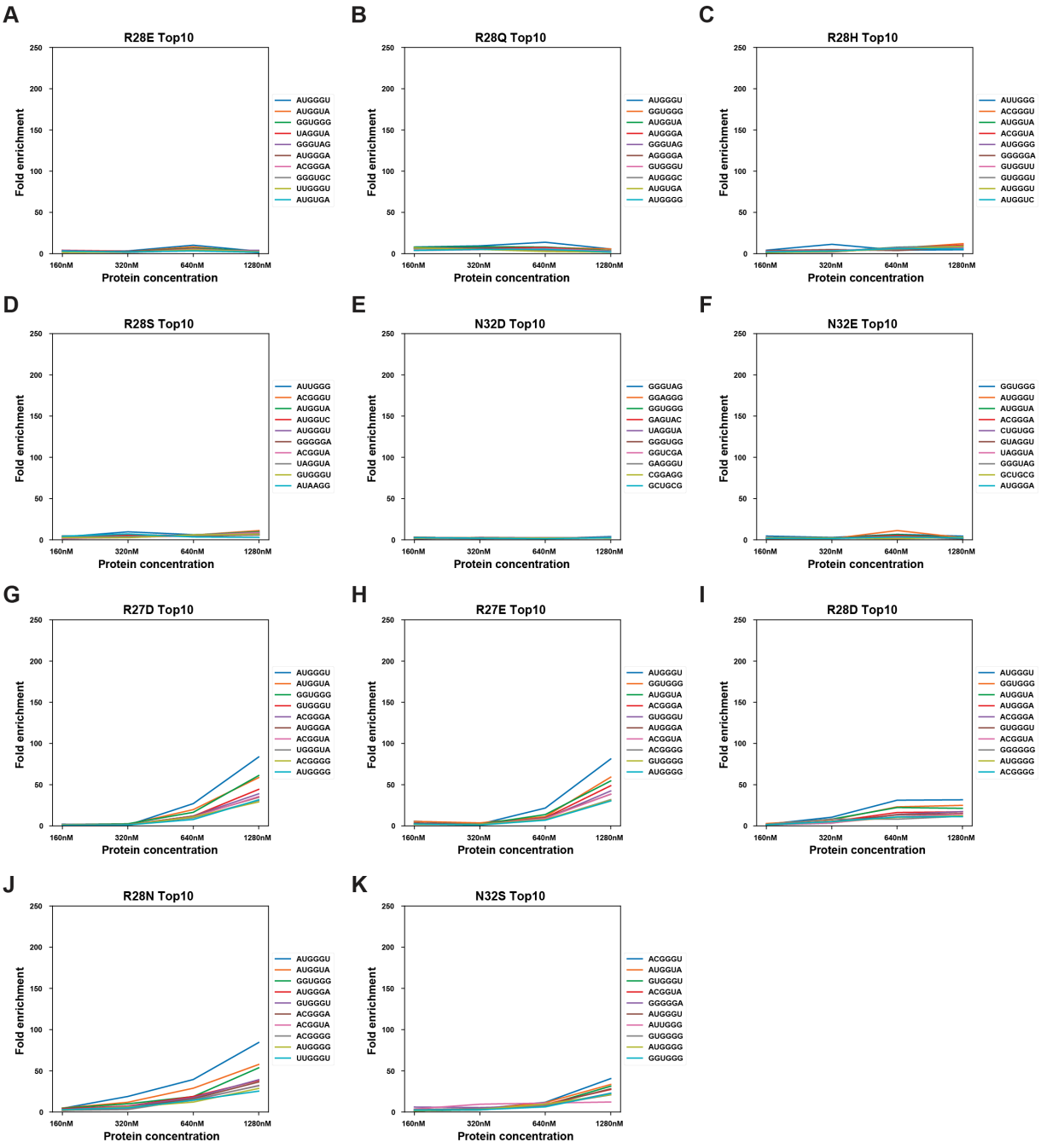

Supplemental Figure S3: Top 10 6-mers in RNA bind-n-seq of other ZnF single mutants with compromised binding affinity

(A-K) Top10 enriched RNA 6-mers of ZnF single mutant R28E, R28Q, R28H, R28S, N32D, N32E, R27D, R27E, R28D, R28N, and N32S.

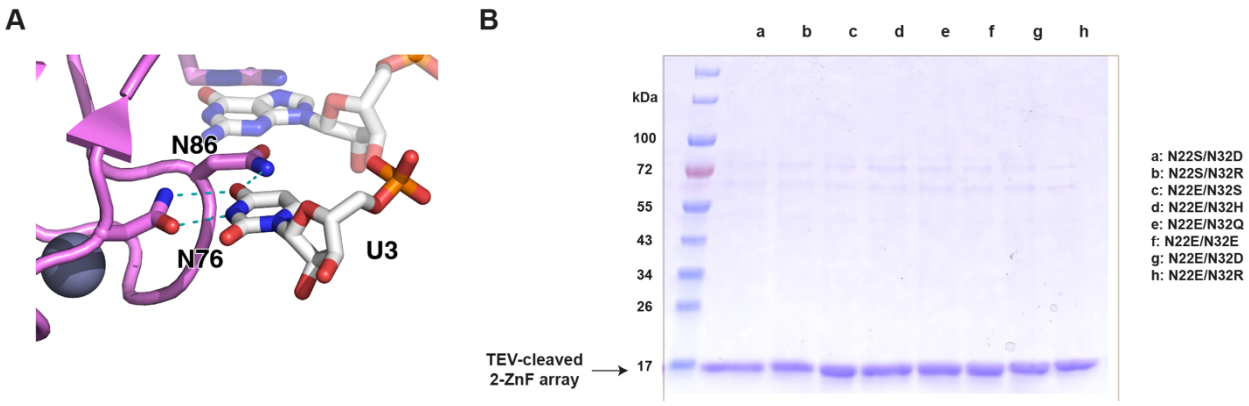

Supplemental Figure S4: Rationale of double mutant ZnF-array design and purification
(A) The interaction between U3 and N76 and N86 (PDB: 3g9y). (B) Representative SDS-PAGE gel image of the high-throughput purification of double mutant ZnF arrays. Note that N22 corresponds to N76 in the ZRANB2 C'-ZnF structure, and N32 corresponds to N86.

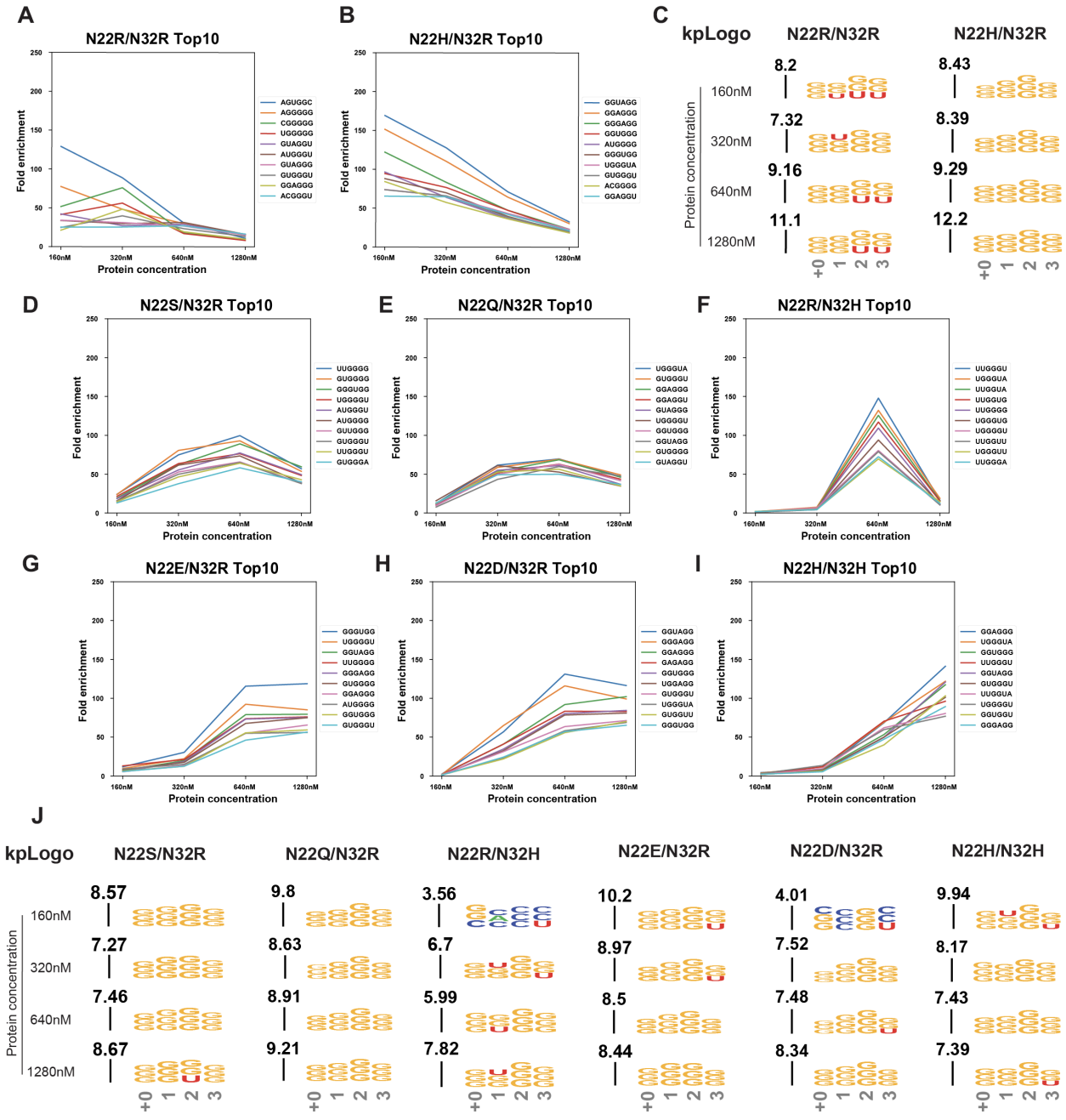

Supplemental Figure S5: RNA bind-n-seq results of selective ZnF double mutants
(A-B) Top10 enriched RNA 6-mers of N22R/N32R and N22H/N32R. This group of double mutants displayed RNA binding specificity to GGU/GGG and retained RNA binding affinity. (C) KpLogo results of N22R/N32R and N22H/N32R. (D-I) Top10 enriched RNA 6-mers of N22S/N32R, N22Q/N32R, N22R/N32H, N22E/N32R, N22D/N32R, and N22H/N32H. This group of double mutants displayed RNA binding specificity to GGG with lower overall RNA binding affinity compared to the wild-type ZnF. (J) KpLogo results of N22S/N32R, N22Q/N32R, N22R/N32H, N22E/N32R, N22D/N32R, and N22H/N32H.

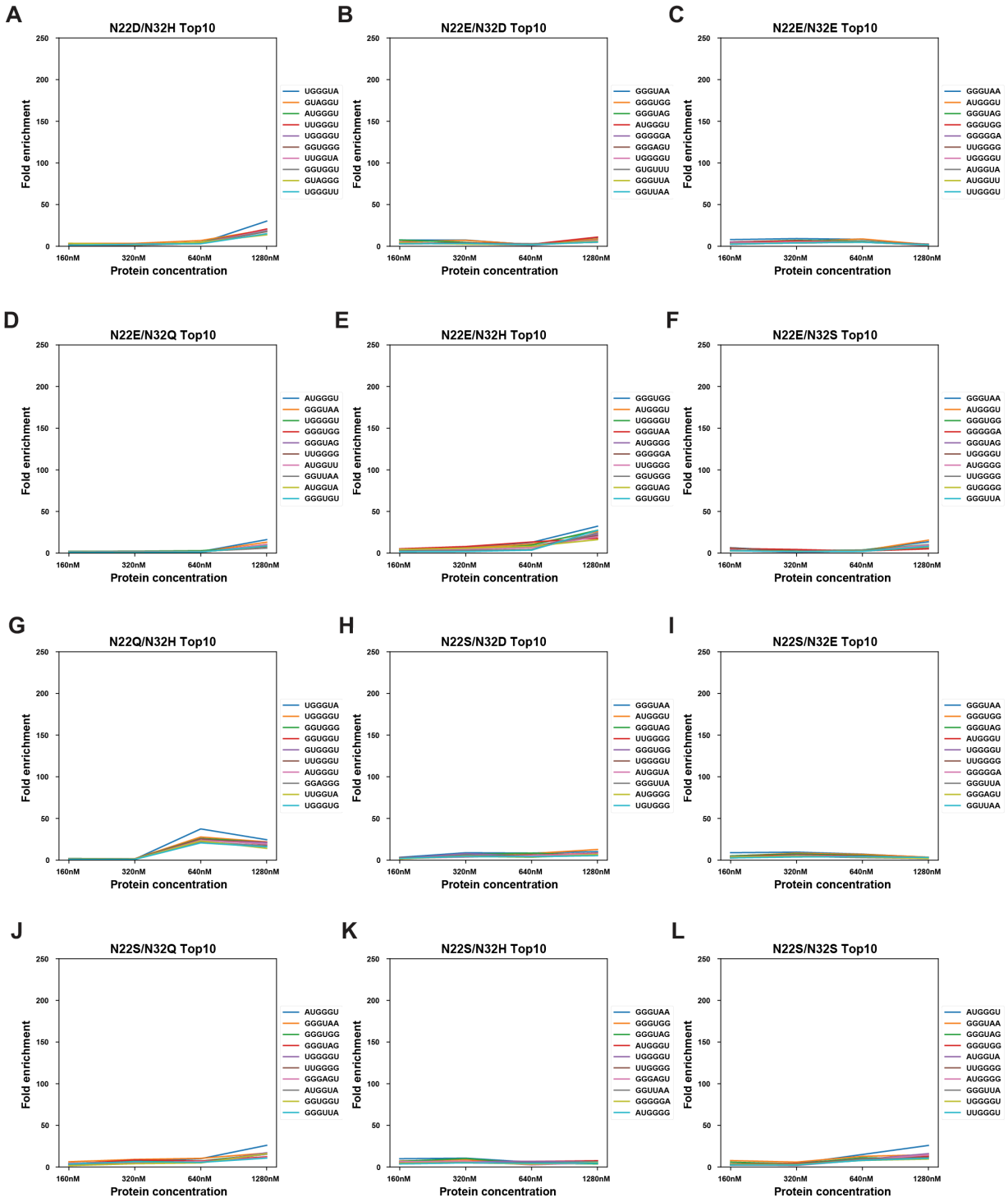

Supplemental Figure S6: Top 10 6-mers in RNA bind-n-seq of ZnF double mutants with compromised binding affinity

(A-L) Top10 enriched RNA 6-mers of ZnF double mutant N22D/N32H, N22E/N32D, N22E/N32E, N22E/N32Q, N22E/N32H, N22E/N32S, N22Q/N32H, N22S/N32D, N22S/N32E, N2S/N32Q, N22S/N32H, and N22S/N32S.

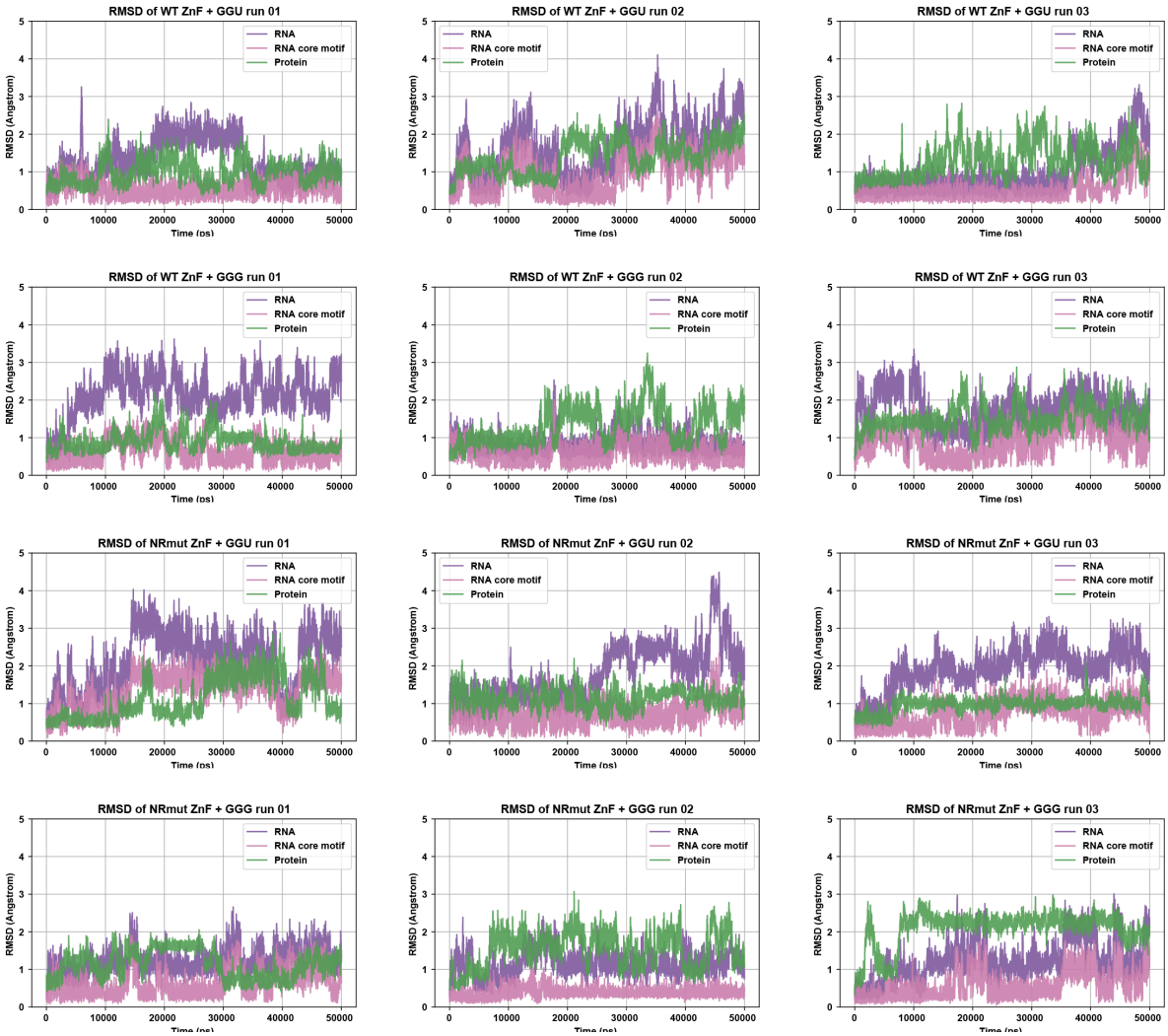

Supplemental Figure S7: Molecular dynamics simulation results of ZnF-RNA complexes
Root mean squared distance (RMSD) of the protein or RNA backbone throughout the simulations, in reference to the equilibrated structure.

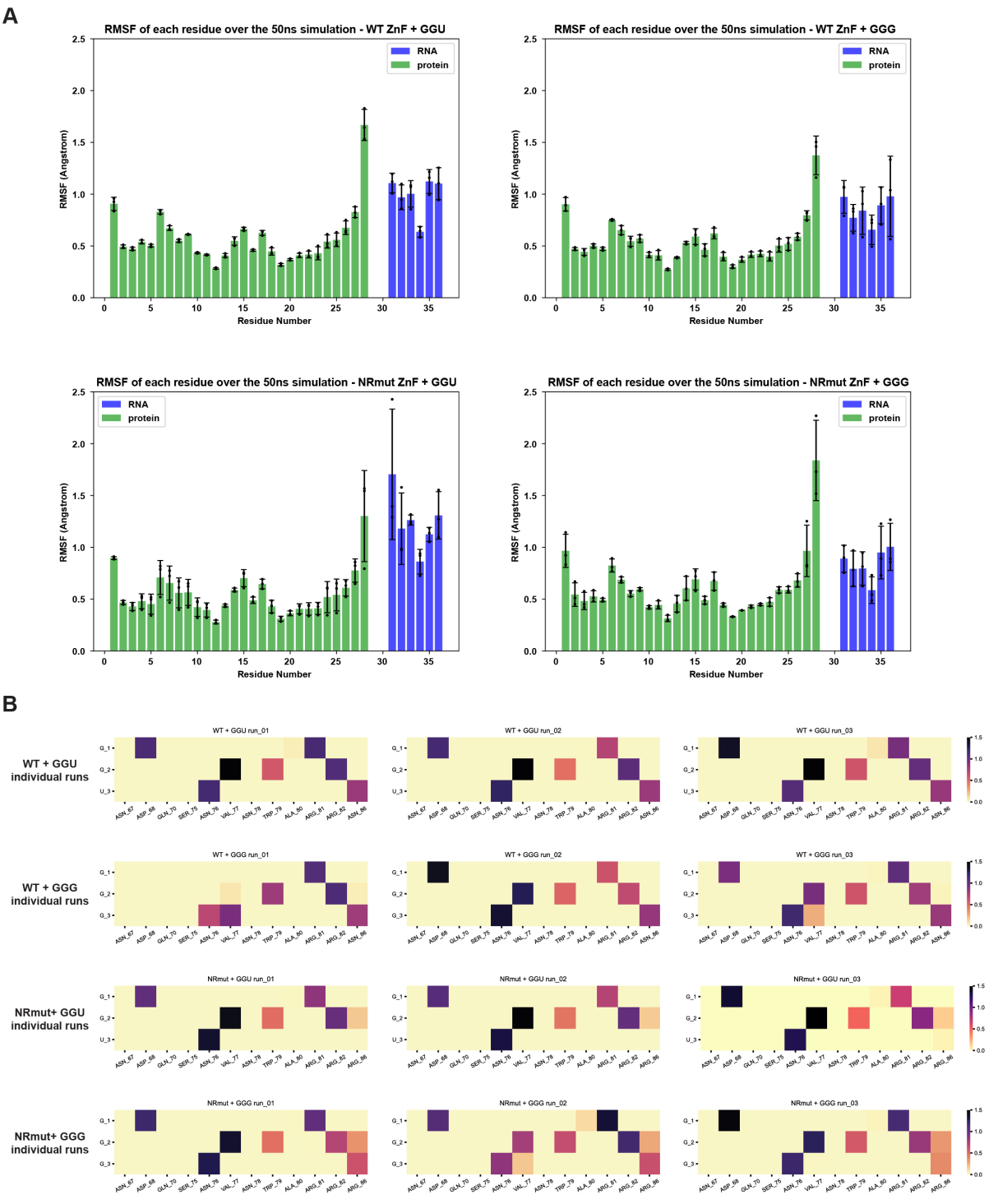

Supplemental Figure S8: Molecular dynamics simulation results of ZnF-RNA complexes (continued)

(A) Root mean squared fluctuation (RMSF) of each protein residue and RNA base during the simulation of in 4 models (ZnF WT + GGU, ZnF WT + GGG, ZnF NRmut + GGU, ZnF NRmut + GGG). Individual replicates are shown, the error bars indicate standard deviations, n=3. (B) Heat map of H-bond intensity between the three RNA bases and the RNA-contacting residues during the simulation. Individual replicates of 50-ns simulations are shown.

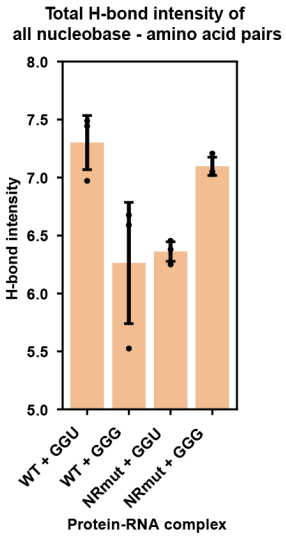

Supplemental Figure S9: Molecular dynamics simulation results of ZnF-RNA complexes (continued)
Total H-bond intensity of all nucleobase-amino acid pairs in 4 models: ZnF WT + GGU, ZnF WT + GGG, ZnF NRmut + GGU, ZnF NRmut + GGG.